Preliminary Deterministic Seismic Landslide Hazard Maps of Tandikat Area

Ruly RESFIANDHI[(1)], Galih W. SWANA[(1)],
Imam A. SADISUN[(1)] and SUMARYONO[(2)]

(1) Bandung Institute of Technology, Indonesia
E-mail: rresfiandhi@gmail.com
(2) Centre for Volcanology and Geological Hazard Mitigation, Indonesia

Abstract

The earthquake with magnitude of 7.6 shook the West Sumatra area and cause of landslides with widespread distribution, therefore needed to conduct a regional analysis of evaluating seismic landslide hazard. Seismic landslide hazard analyses are used to identify, evaluate and assess area hazard of landslides caused by earthquake. These analyses are based on estimates Newmark displacement use deterministic approach with applications of geographic information system tools. The deterministic approach generates different levels of coseismic landslide displacement for given ground motion and critical acceleration, although they are ignoring the uncertainty in these conditions. The expressed of displacements that are predicted via empirical relations equations from combine corresponding of arias intensity and critical acceleration values. The deterministic analysis applied to the Tandikat Quadrangle in Padang Pariaman to develop seismic landslide hazard maps. These maps indicate that deterministic methodology can be applied to define hazard categories.

Keywords: Deterministic, Newmark displacement, seismic landslide, hazard, Tandikat

1. Introduction

The 2009 West Sumatra earthquake had a magnitude 7.6 (M) and epicenter at 99.8°E, 0.79°S with a depth of 74 km in Mentawai Strait, Indonesia. This earthquake caused extensive damage and led to 1,117 fatalities, 2 persons missing, 2,902 person injured, and 249,833 badly damage homes (Bappenas, 2009). The earthquake induced 253 landslides in covering an area 1,500 km^2 (Ueno and Shiiba, 2013) and directly caused at least 130 fatalities (Nakano and Chigira, 2014).

After southern Sumatra earthquake, research on landslide distribution and characteristics was carried out by various authors (e.g., Wang et al., 2010; Ueno and Shiiba, 2013; Faris and Wang, 2014; and Resfiandhi et al., 2014), but, no researchers have mapped and analyzed coseismic landslide in this area. Several methods are used to estimate slope stability during earthquakes, and one of the popular is rigid block (Newmark displacement) analysis which have commonly use deterministic approach.

The medium rainfall event on September 29-30, 2009 (Faris and Wang, 2014), and provided one of the contribution to trigger landslides. Landslides distribution were established by interpretating SPOT image taken after the event. This research is to knowing the estimate Newmark displacement from the West Sumatra earthquake.

2. West Sumatra earthquake

Earthquake with 7.6 Mw shook West Sumatra area on 30 September 2009, at 5:16 pm (fig. 1). McCloskey et al. (2010) said that the earthquake did not cause rupture on Sunda megathrust and did not significantly relax stress accumulation on the Mentawai segment that indicates tsunamigenic earthquake is unabated. The focal mechanism appears an oblique thrust event, but, when viewed in the plane of the plate interface as a slightly oblique strike-slip event.

Wiseman et al. (2012) conducted an investigation with geodetic data and regional seismic that earthquake event is an intraslab earthquake which initiated in the slab subduction process and continuous until 80 km depth, near the plate interface, and produces a ruptured primarily downdip and to the southwest. Based on aftershock distribution and geological context favours to north-south rupture aligns well with the fracture zones on the subducting seafloor.

3. Landslides characteristic

West Sumatra earthquake triggered many landslides in large scale over a wide area. According to Ueno and Shiiba (2013), based on the analysis of satellite imagery using TerraSAR-X, coverage area 1500 km^2 in Padang Pariaman and Agam District show that 253 landslides

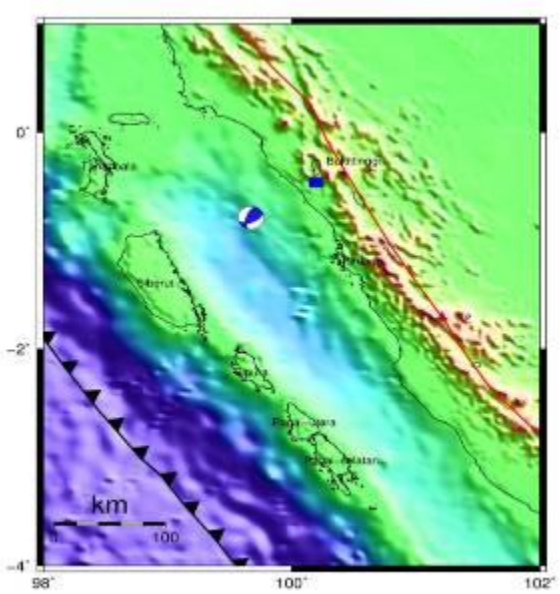

Fig. 1 The 2009 West Sumatra earthquake. The blue rectangle indicates the location area. The focal mechanism (blue-white *'*beach ball*'*) is in map view

had occured with total 70 million m^3 of collapsed sediment. Large scale landslides (volume of sediment > 1 million m^3) are concentrated in Padang Pariaman District which represents 60% of the total volume of sedimentary material that collapsed.

Based on the field investigation, the most common types of landslides triggered by the earthquake were flows and slides of rocks, extending over throughout area and numbered in the hundreds. More disrupted, falls and debris flow, steeper, numbering perhaps tens and occured primarily in the cliff of Maninjau Lake and Anai valley (Photo. 1). The landslides caused more damage and road closures. The most landslides occured primarily on pumice tuff material. According Kastowo et al. (1996), the lithology is hornblende hypersthene pumiceous tuff (Tephra from Tandikat Volcano) consists of pumice lapilli, commonly diameter ranging from 2 to 10 cm, which contain hornblende, hypersthene, and or biotite, moderately compacted, slightly consolidated, loose, easyly collapsed and eroded. The Pumice layers are easily fall, when eroded by rainfall, V-shaped gullies form, the pores are large and interconnected, and hence the permeability of the pumice layer is high (Wang et al., 2010). In addition, there is a hydrothermal alteration process that produces swelling clay effect of clay minerals in the lower part of pumice (Warmada et al., 2010).

Wang et al. (2010) conducted three types of ring shear tests on pumice tuff in the dry and saturated conditions, concluded that the slopes with pumice layer can remain stable in a strong earthquake or during intense rain, but it becomes very unstable when the two events occur simultaneously. It is known that moderate intensity rain occurred several hours before the earthquake event occurred, even recorded that in the the previous night medium rainfall intensity had been going (Faris and Wang, 2014).

4. Location

Determined the location in accordance with area covered of analyzed satellite imagery by Nakano and Chigira (2014) which contain large concentrations of triggered landslides. The rectangle area measured about 94.5 km^2 (fig. 1). The area included northern Padang Pariaman district with flat until moderate slopes areas and Agam district with steep slopes. This area surrounded by Maninjau Lake and Tandikat-Singgalang Volcanoes in northern area and Pariaman City in southern area.

In 2003, the magnitude 3.3 Agam earthquake occured in inland and about 26 km east of location area. That event caused minor damaged homes but the earthquake did not induce landslides.

5. Method

Newmark displacement method is commonly used to analyzed seismic landslide hazard maps. Newmark (1965) introduced model to assess performance slope to estimate displacement. This model as a rigid block that moving downslope when earthquake shaking exceed the block's critical acceleration, and continues until the velocity reach 0. The velocity of rigid block is integrated to result the cumulative displacement. Used deterministic approach to used predicting field displacement for developed seismic landslide hazard maps.

5.1. The static factor of safety

First, computed the static factor of safety which derived from an infinite slope approximation. Static factor of safety can be described as

$$FS = \frac{c'}{\gamma t \sin\alpha} + \frac{\tan\theta'}{\tan\alpha} + \frac{\gamma_w . m \tan\theta'}{\gamma \tan\alpha}$$

where FS is the static factor of safety, c' is the effective cohesion, θ' is effective friction angle, α is slope angle, t is slope normal thickness of failure surface, m is percentage of failure thickness that is saturated, γ is material unit weight, and γ_w is unit weight of water. The shear strength values obtained from field investigation and laboratory test and assigned based on geologic units, although difficult to characterize on a regional basis (Jibson and Michael, 2009). Tabel 1 show the shear strength in the area. For strength data available of each geologic unit, were computed average. Because landslides occured during rainfall conditions, the material on slopes reach saturation. Based on field investigation, the slope thickness of failure surface range from 0.6 to 4.4 m, while saturated thickness from 0.49 to 1.87 m.

(a) (b)

(c) (d)

Photo 1. Landslides triggering by the 2009 West Sumatra earthquake. (a) flow slide, (b) translational slide, (c) debris flow, and (d) rock falls.

We derived slope angle values from 30 m digital elevation model data, although too many topographic irregularities are lost (Jibson et al., 1998, 2000), then, generated in the area has slope angle range from 0° to 62°.

By inserting of shear strength, slab and saturated thickness, and slope angle data, then combining and calculated to get the static of factor safety, We obtained values of static factor of safety range from 0.378 to 10. For further analyzed to model be stable, we assigned factor of safety greater than 1 (fig. 2).

5.2. The critical acceleration

Newmark (1965) showed that critical acceleration can be determined as

$$a_c = (FS - 1)g \sin\alpha$$

where a_c is the critical acceleration, FS is static factor of safety, g is the acceleration of gravity, and α is slope angle. The critical-acceleration map is also seismic landslide susceptibility map, which portrays a measure of intrinsic slope properties independent of any ground-shaking scenario (Jibson et al., 1998, 2000). Critical acceleration in map area until 0.87 g (fig. 3).

5.3. Arias intensity

Arias (1970) intensity measures the total acceleration content of strong motion record. With the lack of data to assigned Arias intensity values in map area, used empirical function from other regions inevitable. Select empirical relationship based on similiar geologic and tectonic of the regions where the equation were made. In this analysis, we used Hsieh et al. (2014) equation. Hsieh et al. developed the Arias intensity equation from subduction earthquakes in

Table 1 Shear strength of geologic units

No.	Unit Name	Formation	c' (KN/m2)	Ø' (°)
1	Sand/silt	Qhpt	28.34	10.92
2	*Mixed layer*	Qhpt	11.47	32.53
3	Paleosol	Qpt	10.20	30.89
4	pumice	Qhpt	33.05	23.91
5	*Mixed layer*	Qhpt	7.65	37.28
6	Paleosol	Qpt	5.10	27.41
7	pumice	Qhpt	5.10	32.96
8	Very fine sand	Qhpt	37.95	22.57
9	Andesite	QTp	11407.03	35.13
10	Andesite	QTp	7194.60	32.48
11	Very coarse sand	Qpt	43.44	25.35
12	Very fine sand	Qpt	28.44	21.72
13	Silt	Qpt	22.75	10.55
14	Lava	Qast	10702.91	36.46
15	Silt	Qast	10.10	10.00
16	mudstone	Qast	22.75	28.91
17	Andesite	Qamj	7072.51	29.38
18	Andesite	Qamj	6861.18	33.48

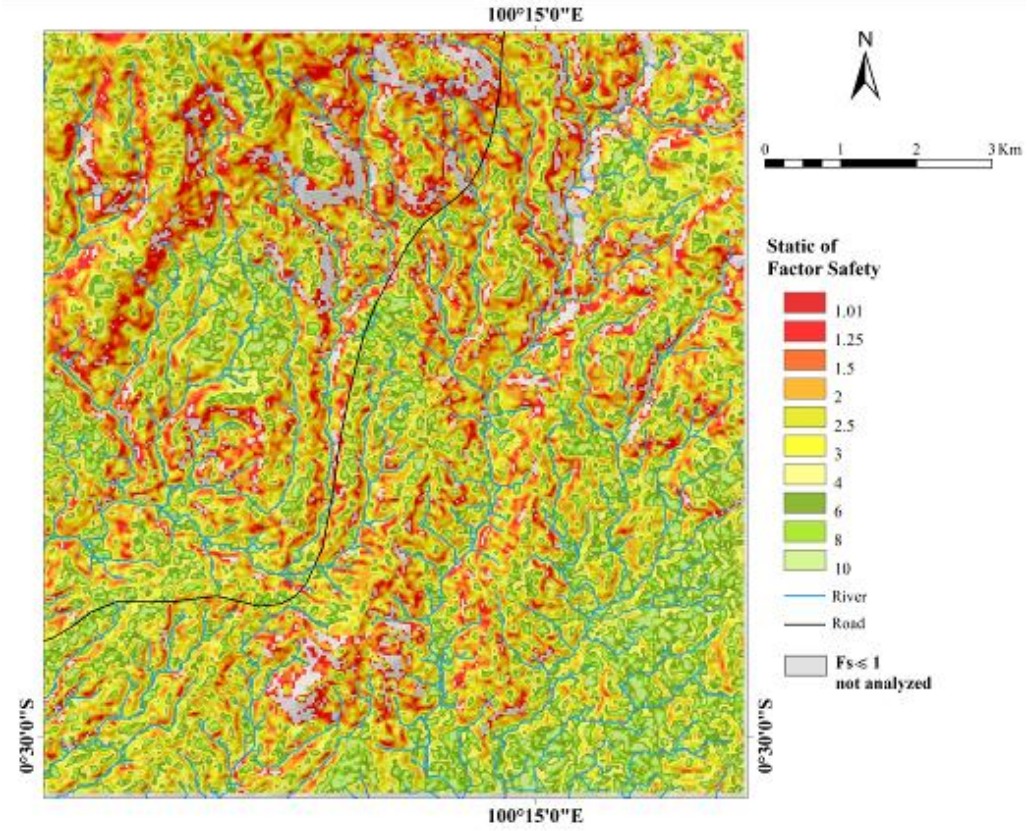

Fig. 2 The static factor of safety map of location

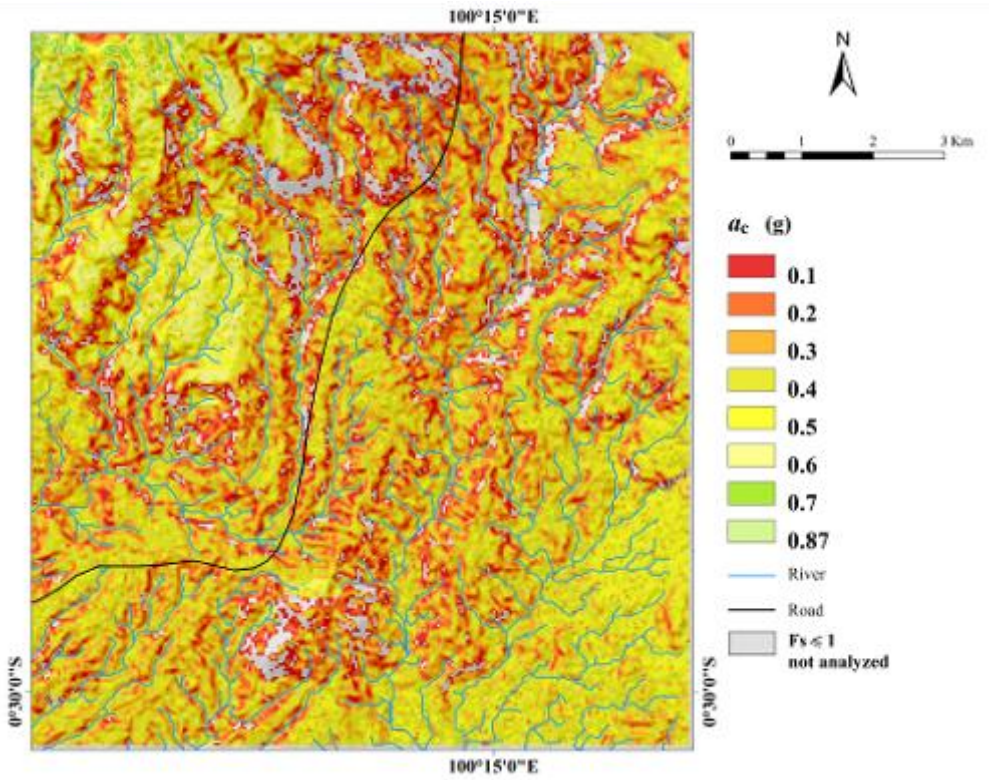

Fig. 3 Critical acceleration map of location. This also map of seismic landslide susceptibility

Taiwan based on strong ground motion. Hsieh et al. defined this equation as

$$\ln Ia = 4{,}357 + 3{,}056\,(M-6) - 2{,}325\,\ln\left(\frac{M}{6}\right) - 2{,}38\,\ln(R) - 0{,}677\,\ln\left({}^{V_{s30}}/_{1130}\right) - 0{,}199\,F_N + 0{,}24\,F_R + 1{,}447\,Zt \pm 0{,}855$$

where M is the moment magnitude of earthquake, R is the hypocentral distance, V_{s30} is shear wave velocity of upper 30 m of material at site, F_N and F_R are dummy variables for the fault types (both being 0 for strike-slip faults, 1, respectively, for normal faults and reverse or reverse oblique faults, and *Zt* indicates the subduction zone earthquake type; *Zt* = 0 for interface earthquakes, and *Zt* = 1 for intraslab earthquakes. We used model based on Wiseman et al. (2012), so the mechanism and type of this earthquake appears as a strike-slip and intraslab, the F_N and F_R are neglected, and for *Zt* value = 1.

Calculated the V_{S30} values based on Matsuoka et al. (2005) methodology, used geomorphologic classification unit as a proxy. This area has V_{S30} values range from 372.1 m/s to 399.9 m/s. According to USGS site classifications, included in site classes C ($760>V_{S30}>360$ m/s), were grouped into rock site category. From calculated those data, then, obtained values of Arias intensity range from 1.47 m/s to 1.71 m/s (fig. 4).

5.4. Newmark displacement

Estimating Newmark displacement method is use empirical regression equation developed from Hsieh and Lee (2011). Hsieh and Lee used strong motion data to refine the relationship among critical acceleration, Arias intensity, and Newmark displacement. The result analyses is developing a set of empirical equations can be used in local (Taiwan) and global, also considered with soil and rock site empirical equation. With assuming could be attributable to relatively similar active orogens or tectonics, the local empirical equation will be applied for this study. We also used rock site local empirical equation to compare the result with all site local empirical equation. Hsieh and Lee defined all site local empirical equation as

$$\log D_n = 0.766\log I_a - 19.945\,a_c + 13.744\,a_c\log I_a + 2.196 \pm 0.458$$

And rock site local empirical equation as

$$\log D_n = 0.555\log I_a - 20.488 a_c + 14.555\,a_c\log I_a + 2.295 \pm 0.414$$

where D_n is Newmark displacement, Ia is Arias intensity, and a_c is critical acceleration. The goodness of fit for all site local empirical and rock site local empirical equation are $R^2 = 0.837$ and $R^2 = 0.875$.

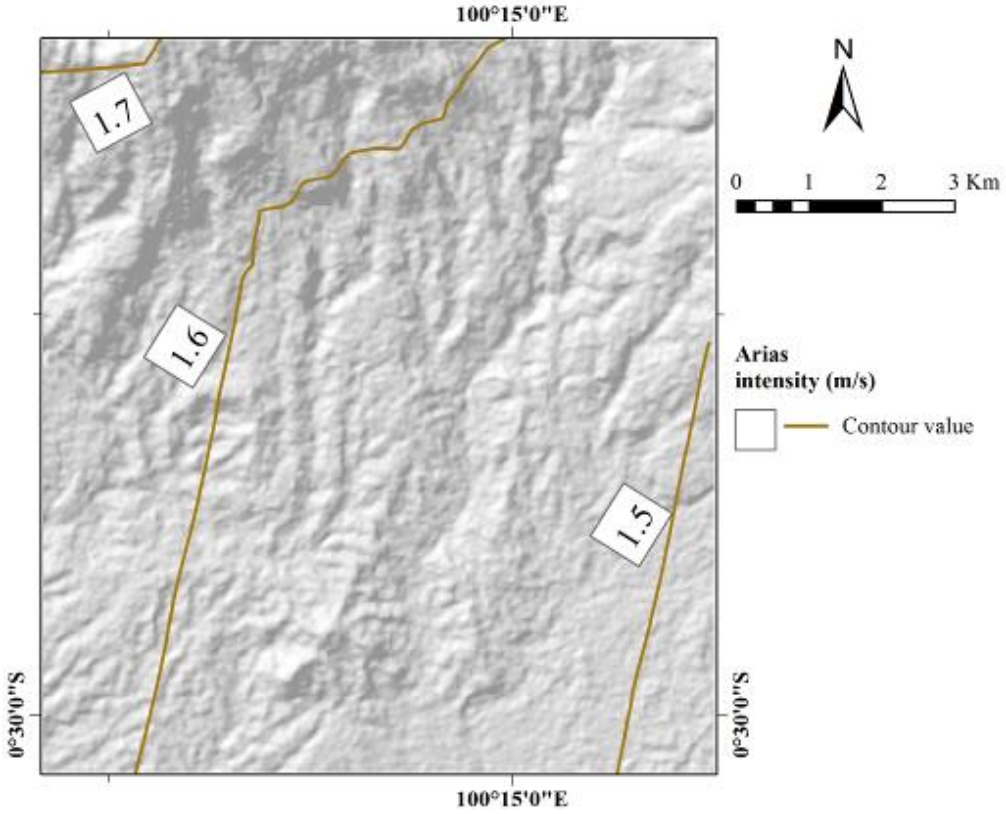

Fig. 4 Contours of Arias intensity map of location. This map generated by Hsieh et al. (2014) equation

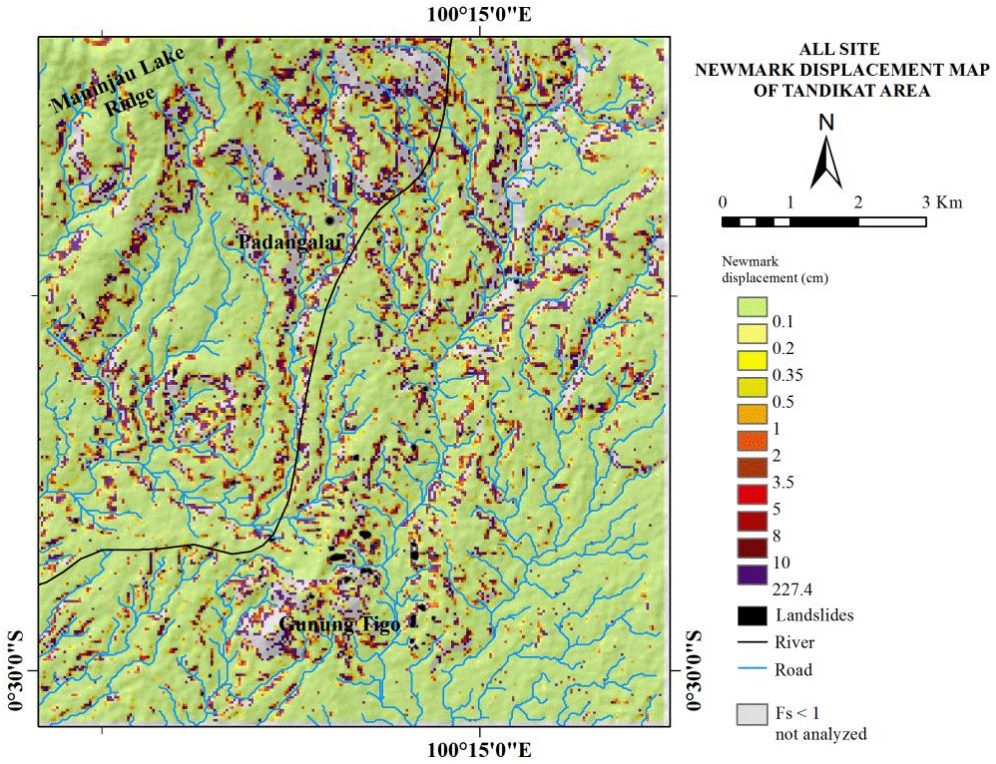

Fig. 5 Predicted Newmark displacement map. This map generated by Hsieh and Lee (2011) all site equation.

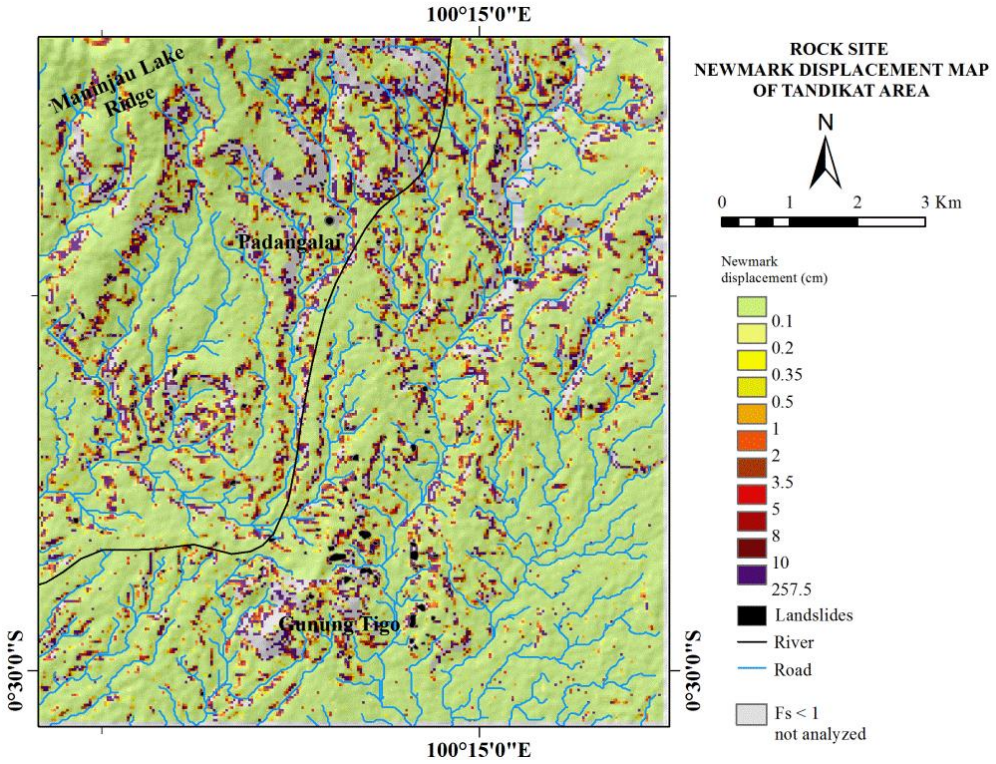

Fig. 6 Predicted Newmark displacement map. This map generated by Hsieh and Lee (2011) rock site local equation

Estimated Newmark displacement range from 0 to 227.4 cm for all site local equation (fig. 5), and 0 to 257.5 for rock site local equation (fig. 6).

6. Conclusions

The result declare that relative similiar displacement between all site and rock site. However, the rock site result is higher value than the all site result. This result is appropriate with demonstrated the developed of equation.

The methods ignored the static factor of safety less than 1. This constraint in order to be model statically stable. So, assigning shear strength, material unit weight data, and determine slab thickness and saturated slab is subjective process.

Although used simplified approach, this procedure could be used for analysis seismic landslide hazard if source of geometry, shear strength data, V_{s30} value, are known. The next step is predicting the probability of failure using inventories of landslides triggered by earthquake. This is the near future work.

Acknowledgments

The authors are grateful to the Centre for Volcanology and Geological Hazard Mitigation provided material shear strengths and V_{S30} data. Randal W. Jibson and Chyi-Tyi Lee helpful insights for expertise regarding the method. Jewgenij Torizin and Randy Kartiko provided helpful insights to modeling.

References

Arias, A. (1970): A measure of earthquake intensity. In: Hansen, R.J. (Ed.), Seismic Design for Nuclear Power Plants, Massachusetts Institute of Technology Press, Cambridge, MA, pp. 438–483.

Bappenas. (2009): Rencana Aksi Rehabilitasi dan Rekonstruksi Wilayah Pascabencana Gempabumi di Provinsi Sumatra Barat Tahun 2009 – 2011, Kementerian Negara Perencanaan Pembangunan Nasional/ Badan Perencanaan Pembangunan Nasional, 135 p.

Faris, F. and Wang, F. (2014): Investigation of the initiation mechanism of an earthquake- induced landslide during rainfall: a case study of the Tandikat landslide, West Sumatra, Indonesia, Geoenvironmental Disaster, 1:4, pp. 1-18.

Hsieh, S.-Y. and Lee, C.-T. (2011): Empirical estimation of the Newmark displacement from the Arias intensity and critical acceleration, Engineering Geology, 122, pp. 34–42.

Hsieh, P.-S., Lin, P.-S., Cheng, C.-T., and Lee, C.-T. (2014): New Predictive Equation for Arias Intensity from Subduction Earthquakes in Taiwan, Sinotech Engineering, Vol. 125, pp. 33-43.

Jibson, R.W., Harp, E.L., and Michael, J.A. (1998): A method for producing digital probabilistic seismic landslide hazard maps—an example from the Los Angeles, California, area, U.S. Geological Survey Open-File Report 98–113, 2 pl., 17 p.

Jibson, R.W., Harp, E.L., and Michael, J.A. (2000): A method for producing digital probabilistic seismic

landslide hazard maps, Engineering Geology, 58, pp. 271–289.

Jibson, R.W. and Michael, J.A. (2009): Maps showing seismic landslide hazards in Anchorage, Alaska, U.S. Geological Survey Scientific Investigations Map 3077, 2 sheets (scale 1:25, 000), 11 p.

Kastowo, Leo, G.W., Gafoer, S., and Amin, T.C. (1996): Geological map of the Padang Quadrangle, Sumatra, Scale 1 : 250,000. Geological Research and Development Centre.

Matsuoka, M., Wakamatsu, K., Fujimoto, K., and Midorikawa, S. (2005): Nationwide site amplification zoning using GIS-based Japan Engineering Geomorphologic Classification Map, In: 9th International Conference on Structural Safety and Reliability, Rome, pp. 239-246.

McCloskey, J., Lange, D., Tilmann, F., Nalbant, S.S., Bell, A.F., Natawidjaja, D.H., and Rietbrock, A. (2010): The September 2009 Padang earthquake, Nature Geoscience,Vol. 3, pp. 70–71.

Nakano, M. and Chigira, M. (2014): Geomorphological and Geological Features of the Collapsing Landslides Induced by the 2009 Padang Earthquake. Japan Geoscience Union Meeting 2014.

Newmark, N.M. (1965): Effects of earthquakes on dams and embankments. Geotechnique, 15, pp. 139–159.

Resfiandhi, R., Sumaryono, and Sadisun, I.A. (2014): Karakteristik Longsoran yang Disebabkan Gempabumi Sumatra Barat Berdasarkan Penginderaan Jauh, Proceedings The 43rd IAGI Annual Convention and Exhibition, Jakarta.

Ueno, T. and Shiiba, S. (2013): Landslides in Padang, West Sumatra, Triggered by the September 2009 Offshore Earthquake, Internasional Journal of Erosion Control Engineering, Vol. 6, No. 1, pp.30-36.

Wang, F., A.N. Wafid, M., and Zhang, F. (2010): Tandikek and Malalak flowslides triggered by 2009.9.30 M7.6 Sumatra earthquake during rainfall in Indonesia. Geoscience Rept. Shimane Univ, 29, pp. 1-10.

Warmada, I.W., Wilopo, W., and Harijoko, A. (2010): Mineralogical control on landslide in strongly weathered volcanic terrain. Case study: Padang Pariaman, West Sumatra, Proceedings of The International Symposium and 2nd AUN/Seed-Net Regional Conference on Geo-Disaster Mitigation in ASEAN 2010.

Wiseman, K., Banerjee, P., Bürgmann, R., Sieh, K., Dreger, D.S., and Hermawan I. (2012): Source model of the 2009*M*w 7.6 Padang intraslab earthquake and its effect on the Sunda megathrust, Geophysical Journal International, 190, pp. 1710-1722.

.